COMPARISON OF MULTIPLE-MICROPHONE AND SINGLE-LOUDSPEAKER ADAPTIVE FEEDBACK/ECHO CANCELLATION SYSTEMS

Meng Guo[1,2]*, Thomas Bo Elmedyb*[1]*, Søren Holdt Jensen*[2]*, and Jesper Jensen*[1]

[1]Oticon A/S, Kongebakken 9, DK-2765 Smørum, Denmark
[2]Department of Electronic Systems, Aalborg University, Niels Jernes Vej 12, DK-9220 Aalborg, Denmark
emails: {guo, tbn, jsj}@oticon.dk, shj@es.aau.dk

ABSTRACT

Recently, we introduced a frequency domain measure - the power transfer function - to predict the convergence rate, system stability bound and the steady-state behavior across time and frequency of a least mean square based feedback/echo cancellation algorithm in a general multiple-microphone and single-loudspeaker system. In this work, we extend the theoretical analysis to the normalized least mean square and recursive least squares algorithms. Furthermore, we compare and discuss the system behaviors in terms of the power transfer function for all three adaptive algorithms.

1. INTRODUCTION

Acoustic feedback/echo problems occur when the microphone of a sound system picks up the acoustic output signal from its own loudspeaker. In practical applications such as public address systems, teleconferencing systems and hearing aids, the acoustic feedback/echo problem can cause significant degradation of the system performance.

Feedback/echo cancellation by means of adaptive filters is one of the most widely used methods to deal with the acoustic feedback/echo problem, see e.g. [1, 2] and the references therein. A range of different adaptive algorithms have been proposed including the least mean square (LMS), normalized least mean square (NLMS), affine projection (AP), and the recursive least squares (RLS) algorithms to mention a few [3].

Some of the most widely used criteria for designing and evaluating the adaptive filters are based on the mean-square error and mean-square deviation, see e.g. [3]. Although very useful, they are typically time domain criteria. On the other hand, the acoustic feedback/echo paths from the loudspeaker to the microphones are often easier described in the frequency domain by magnitude and phase spectra. Hence, one could argue that a frequency domain measure might be more suitable as a design and evaluation criterion.

Recently, we proposed a new frequency domain design and evaluation criterion - the power transfer function (PTF) - and analyzed a multiple-microphone and single-loudspeaker (MMSL) system with a beamformer [4], as shown in Fig. 1, where the PTF is defined as the expected magnitude-squared transfer function from point A to B. Such an MMSL system could be a teleconferencing system, a headset system or a typical hearing aid system. In [4], the LMS algorithm was applied in the adaptive cancellation systems to estimate $\hat{\mathbf{h}}_i(n)$ used for cancelling the acoustic feedback/echo paths $\mathbf{h}_i(n)$. Furthermore, the PTF is directly related to the cancellation system performance: with a perfect cancellation, i.e. $\hat{\mathbf{h}}_i(n) = \mathbf{h}_i(n)$, the PTF equals to zero for all frequencies. The analysis was inspired by the work in [5], where a single-microphone and single-loudspeaker system was analyzed.

In this work, we extend our previous analysis [4] of the acoustic feedback/echo cancellation in the MMSL system to cover the NLMS and RLS algorithms. We derive analytical expressions for the PTF for these two adaptive algorithms. Furthermore, we compare the system behaviors, in terms of the convergence rate and steady-state behavior, across time and frequency, for all three adaptive algorithms, namely the LMS, NLMS and the RLS algorithms.

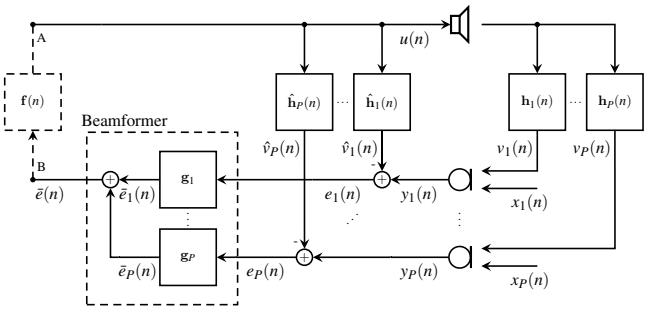

Figure 1: The multiple-microphone and single-loudspeaker system. The power transfer function describes the expected magnitude-squared transfer function from point A to B.

In this paper, column vectors and matrices are emphasized using lower and upper letters in bold, respectively. Transposition, Hermitian transposition and complex conjugation are denoted by the superscripts T, H and $*$, respectively.

2. SYSTEM DESCRIPTION

In this section, we introduce the MMSL system shown in Fig. 1.

The true but unknown feedback path from the loudspeaker to the i'th microphone is modeled by a finite impulse response (FIR) of order $L-1$,

$$\mathbf{h}_i(n) = [h_i(0,n), \ldots, h_i(L-1,n)]^T. \tag{1}$$

The frequency response as the discrete Fourier transform (DFT) of $\mathbf{h}_i(n)$ is expressed by

$$H_i(\omega,n) = \sum_{k=0}^{L-1} h_i(k,n) e^{-j\omega k}. \tag{2}$$

As in [5], we model time variations of the true feedback paths $\mathbf{h}_i(n)$ using a random walk model

$$H_i(\omega,n) = H_i(\omega,n-1) + \check{H}_i(\omega,n), \tag{3}$$

where $\check{H}_i(\omega,n) \in \mathbb{C}$ is a sample from a zero-mean Gaussian white noise process with variance

$$S_{\check{h}_{ii}}(\omega) = E\left[\check{H}_i(\omega,n)\check{H}_i^*(\omega,n)\right]. \tag{4}$$

In the time domain, the feedback path variation vector is

$$\check{\mathbf{h}}_i(n) = \mathbf{h}_i(n) - \mathbf{h}_i(n-1). \tag{5}$$

The correlation matrix of the i'th and j'th feedback path variations is given by

$$\check{\mathbf{H}}_{ij} = E\left[\check{\mathbf{h}}_i(n)\check{\mathbf{h}}_j^T(n)\right], \tag{6}$$

and we assume, for simplicity, that $\check{\mathbf{H}}_{ij} = \mathbf{0}_{L\times L}$ for $i \neq j$.

The estimate $\hat{\mathbf{h}}_i(n)$ of the i'th true feedback path is

$$\hat{\mathbf{h}}_i(n) = \left[\hat{h}_i(0,n),\ldots,\hat{h}_i(L-1,n)\right]^T, \tag{7}$$

and the corresponding estimation error vector is defined as

$$\tilde{\mathbf{h}}_i(n) = \hat{\mathbf{h}}_i(n) - \mathbf{h}_i(n), \tag{8}$$

with a frequency response of

$$\tilde{H}_i(\omega,n) = \sum_{k=0}^{L-1} \tilde{h}_i(k,n)e^{-j\omega k}. \tag{9}$$

Each beamformer filter $\mathbf{g}_i$, to perform the spatial filtering, is represented by an FIR filter

$$\mathbf{g}_i = [g_i(0),\ldots,g_i(N-1)]^T, \tag{10}$$

and its frequency response is expressed by

$$G_i(\omega) = \sum_{k=0}^{N-1} g_i(k)e^{-j\omega k}. \tag{11}$$

The loudspeaker signal vector $\mathbf{u}(n)$ is defined as

$$\mathbf{u}(n) = [u(n),\ldots,u(n-L+1)]^T. \tag{12}$$

We consider the loudspeaker signal $u(n)$ as a zero-mean deterministic signal because it is measurable and thereby known in the analysis. However, as argued in [5], our results remain valid, even if the loudspeaker signal $u(n)$ is considered as a realization of a stochastic process, which is statistically independent of the incoming signals $x_i(n)$. Thus, we define the deterministic autocorrelation matrix

$$\mathbf{R}_u(k) = \lim_{N\to\infty} \frac{1}{N} \sum_{n=1}^{N} \mathbf{u}(n)\mathbf{u}^T(n-k). \tag{13}$$

We assume that the incoming signals $x_i(n)$ are zero-mean, stationary stochastic signals with correlation function

$$r_{x_{ij}}(k) = E\left[x_i(n)x_j(n-k)\right]. \tag{14}$$

Furthermore, the i'th microphone signal $y_i(n)$ is modeled as

$$y_i(n) = \mathbf{h}_i^T(n-1)\mathbf{u}(n) + x_i(n). \tag{15}$$

The i'th error signal $e_i(n)$ is given by

$$e_i(n) = y_i(n) - \hat{\mathbf{h}}_i^T(n-1)\mathbf{u}(n). \tag{16}$$

The beamformer output signal $\bar{e}(n)$ is expressed by

$$\bar{e}(n) = \sum_{i=1}^{P} \bar{e}_i(n) = \sum_{i=1}^{P}\sum_{k=0}^{N-1} g_i(k)e_i(n-k). \tag{17}$$

In acoustic echo cancellation (AEC) applications such as teleconferencing systems, the forward path $\mathbf{f}(n)$ denotes the far-end transfer function. Assuming an echo cancellation algorithm is applied at the far-end, $\mathbf{f}(n) \approx \mathbf{0}$ in this case, these systems would effectively be operating in a open-loop setup.

On the other hand, in acoustic feedback cancellation (AFC) applications such as public address systems and hearing aids, the forward path $\mathbf{f}(n)$ can not be ignored, thus, these systems are operating in a closed-loop setup.

Although we consider the open-loop setup in our analysis, as argued in Sec. 3, the results are highly relevant for the closed-loop setup as well.

3. REVIEW OF POWER TRANSFER FUNCTION

The PTF describes the expected magnitude-squared transfer function from point A to B in Fig. 1. The frequency responses $H_i(\omega,n)$ of the true feedback paths $\mathbf{h}_i(n)$ are unknown and considered as stochastic. Hence, as in [4], we define the exact PTF of the MMSL system as

$$\begin{aligned}\xi(\omega,n) &= E\left[\left|\sum_{i=1}^{P} G_i(\omega)\tilde{H}_i(\omega,n)\right|^2\right] \\ &= \sum_{i=1}^{P}\sum_{j=1}^{P} G_i(\omega)G_j^*(\omega)\xi_{ij}(\omega,n),\end{aligned} \tag{18}$$

where $\xi_{ij}(\omega,n) = E[\tilde{H}_i(\omega,n)\tilde{H}_j^*(\omega,n)]$.

Thus, the PTF $\xi(\omega,n)$ describes the cancellation performance over time and frequency, not only for one particular cancellation filter as e.g. the criterion mean-square deviation $E[\|\tilde{\mathbf{h}}(n)\|^2]$, but for the entire system.

For closed-loop AFC systems, the PTF $\xi(\omega,n)$ is part of the expected magnitude-squared open-loop transfer function $E[|\mathrm{OLTF}(\omega,n)|^2]$ of the MMSL system expressed by $E\left[|\mathrm{OLTF}(\omega,n)|^2\right] = |F(\omega,n)|^2\xi(\omega,n)$, where $F(\omega,n)$ denotes the frequency response of the forward path $\mathbf{f}(n)$. If $|\mathrm{OLTF}(\omega,n)|^2 < 1$, system stability is guaranteed [6].

In this way, by estimating the PTF $\xi(\omega,n)$, we identify the unknown part of $E[|\mathrm{OLTF}(\omega,n)|^2]$. Furthermore, given a desired value of $E[|\mathrm{OLTF}(\omega,n)|^2]$, we could determine the maximum allowed forward path magnitude to ensure system stability as $|F(\omega,n)| < 1/\sqrt{\xi(\omega,n)}$.

In general, however, we can not calculate the PTF $\xi(\omega,n)$ directly because $H_i(\omega,n)$ is unknown. In this work, we derive a simpler but accurate approximation of the PTF as

$$\hat{\xi}(\omega,n) = \sum_{i=1}^{P}\sum_{j=1}^{P} G_i(\omega)G_j^*(\omega)\hat{\xi}_{ij}(\omega,n), \tag{19}$$

where

$$\hat{\xi}_{ij}(\omega,n) \approx E\left[\tilde{H}_i(\omega,n)\tilde{H}_j^*(\omega,n)\right]. \tag{20}$$

4. SYSTEM ANALYSIS

4.1 Review of PTF for LMS Algorithm

In [4], we considered an MMSL system where the feedback paths $\mathbf{h}_i(n)$ were estimated using the LMS algorithm. We showed that, under the assumptions of the LMS step size $\mu_0(n) \to 0$, the length of estimation filter $L \to \infty$ and $r_{x_{ij}}(k) = 0\ \forall\ |k| > k_0 \in \mathbb{N}$, the PTF could be approximated as

$$\begin{aligned}\hat{\xi}(\omega,n) &= (1-2\mu_0(n)S_u(\omega))\,\hat{\xi}(\omega,n-1) \\ &\quad + L\mu_0^2(n)S_u(\omega)\sum_{i=1}^{P}\sum_{j=1}^{P} G_i(\omega)G_j^*(\omega)S_{x_{ij}}(\omega) \\ &\quad + \sum_{i=1}^{P} |G_i(\omega)|^2 S_{\check{h}_{ii}}(\omega),\end{aligned} \tag{21}$$

where $S_u(\omega)$ denotes the power spectrum density (PSD) of the loudspeaker signal $u(n)$, and $S_{x_{ij}}(\omega)$ denotes the cross(auto) PSDs of the incoming signals $x_i(n)$ and $x_j(n)$.

Furthermore, by considering Eq. (21) as a first-order difference equation in $\hat{\xi}(\omega,n)$, the convergence rate describing the decay of $\hat{\xi}(\omega,n)$ is expressed by the coefficient

$$\alpha = 1 - 2\mu_0(n)S_u(\omega), \tag{22}$$

which determines the pole location of the first-order system.

The convergence rate in dB/iteration is expressed by

$$\mathrm{CR[dB/iteration]} = 10\log_{10}\alpha. \tag{23}$$

Furthermore, system stability is ensured if

$$|\alpha| < 1. \tag{24}$$

From Eq. (21), the steady-state behavior, in terms of a steady-state error and a tracking error, when $\hat{\xi}(\omega,n)$ has converged, is

$$\begin{aligned}\hat{\xi}(\omega,\infty) &= \lim_{n\to\infty}\hat{\xi}(\omega,n)\\ &= \underbrace{\lim_{n\to\infty} L\frac{\mu_0(n)}{2}\sum_{i=1}^{P}\sum_{j=1}^{P} G_i(\omega)G_j^*(\omega)S_{x_{ij}}(\omega)}_{\text{Steady-State Error}}\\ &\quad + \underbrace{\lim_{n\to\infty}\frac{\sum_{i=1}^{P}|G_i(\omega)|^2 S_{\check{h}_{ii}}(\omega)}{2\mu_0(n)S_u(\omega)}}_{\text{Tracking Error}}.\end{aligned} \tag{25}$$

4.2 PTF for NLMS Algorithm

When using the NLMS algorithm, the update of the i'th microphone channel is, see e.g. [3],

$$\hat{\mathbf{h}}_i(n) = \hat{\mathbf{h}}_i(n-1) + \mu(n)\frac{\mathbf{u}(n)e_i(n)}{\mathbf{u}^T(n)\mathbf{u}(n)+\delta}, \tag{26}$$

where $\mu(n)$ is the NLMS step size, and $\delta > 0$ is a small positive number often referred to as the regularization term. In the following, we neglect this term because its function is to avoid numerical instability. Furthermore, using the assumption of $\mu(n) \to 0$, we can rewrite Eq. (26) as

$$\hat{\mathbf{h}}_i(n) = \hat{\mathbf{h}}_i(n-1) + \mu(n)\frac{\mathbf{u}(n)e_i(n)}{L\sigma_u^2}, \tag{27}$$

where σ_u^2 is the variance of the loudspeaker signal $u(n)$.

Now, from Eq. (27), we can see that the estimation of $\hat{\mathbf{h}}_i(n)$ is equivalent to the LMS algorithm with an adjusted step size as

$$\mu_0(n) = \frac{\mu(n)}{L\sigma_u^2}. \tag{28}$$

Hence, inserting Eq. (28) in Eq. (21), we can express the PTF estimate $\hat{\xi}(\omega,n)$ of the MMSL system, when using the NLMS algorithm under the assumptions of $\mu(n) \to 0$, $L \to \infty$ and $r_{x_{ij}}(k) = 0\ \forall\ |k| > k_0 \in \mathbb{N}$, as

$$\begin{aligned}\hat{\xi}(\omega,n) &= \left(1 - 2\frac{\mu(n)}{L\sigma_u^2}S_u(\omega)\right)\hat{\xi}(\omega,n-1)\\ &\quad + \frac{\mu^2(n)}{L\sigma_u^4}S_u(\omega)\sum_{i=1}^{P}\sum_{j=1}^{P} G_i(\omega)G_j^*(\omega)S_{x_{ij}}(\omega)\\ &\quad + \sum_{i=1}^{P}|G_i(\omega)|^2 S_{\check{h}_{ii}}(\omega).\end{aligned} \tag{29}$$

4.3 PTF for RLS Algorithm

Using the RLS algorithm, the cost function of the i'th microphone channel is expressed by, see e.g. [3],

$$J_i(n) = \sum_{m=1}^{n}\lambda^{n-m}e_i^2(m), \tag{30}$$

where $0 < \lambda < 1$ denotes the forgetting factor, and the RLS update step is expressed by

$$\hat{\mathbf{h}}_i(n) = \hat{\mathbf{h}}_i(n-1) + \mathbf{Z}(n)\mathbf{u}(n)e_i(n), \tag{31}$$

where

$$\mathbf{Z}(n) = \frac{\mathbf{P}(n-1)}{\lambda + \mathbf{u}^T(n)\mathbf{P}(n-1)\mathbf{u}(n)}, \tag{32}$$

and

$$\mathbf{P}(n) = \frac{1}{\lambda}\left(\mathbf{P}(n-1) - \mathbf{Z}(n)\mathbf{u}(n)\mathbf{u}^T(n)\mathbf{P}(n-1)\right). \tag{33}$$

$\mathbf{P}(0)$ is typically chosen as $\mathbf{P}(0) = \delta\mathbf{I}$, where δ is a regularization parameter.

Using Eqs. (31), (16), (15) and (5), the estimation error vector defined in Eq. (8) can be expressed by

$$\begin{aligned}\tilde{\mathbf{h}}_i(n) &= \left(\mathbf{I} - \mathbf{Z}(n)\mathbf{u}(n)\mathbf{u}^T(n)\right)\tilde{\mathbf{h}}_i(n-1)\\ &\quad + \mathbf{Z}(n)\mathbf{u}(n)x_i(n) - \check{\mathbf{h}}_i(n),\end{aligned} \tag{34}$$

where $\mathbf{I}$ is the identity matrix.

We can show, under the assumption of $\lambda \to 1$ and $r_{x_{ij}}(k) = 0\ \forall\ |k| > k_0 \in \mathbb{N}$, that an approximation of the estimation error correlation matrix $\mathbf{H}_{ij}(n) = E[\tilde{\mathbf{h}}_i(n)\tilde{\mathbf{h}}_j^T(n)]$ is expressed by

$$\begin{aligned}\hat{\mathbf{H}}_{ij}(n) &= \hat{\mathbf{H}}_{ij}(n-1) - \mathbf{Z}(n)\mathbf{R}_u(0)\hat{\mathbf{H}}_{ij}(n-1)\\ &\quad - \hat{\mathbf{H}}_{ij}(n-1)\mathbf{R}_u(0)\mathbf{Z}^T(n)\\ &\quad + \sum_{k=-k_0}^{k_0}\mathbf{Z}(n)\mathbf{R}_u(k)\mathbf{Z}^T(n)r_{x_{ij}}(k) + \check{\mathbf{H}}_{ij}.\end{aligned} \tag{35}$$

Now, we use the DFT matrix $\mathbf{F} \in \mathbb{C}^{L\times L}$ to diagonalize the Toeplitz matrix $\hat{\mathbf{H}}_{ij}(n)$ as $L \to \infty$ [7]. We can show that each element in the diagonal of the resulting matrix is

$$\begin{aligned}\hat{\xi}_{ij}(\omega,n) &= (1 - 2z(\omega,n)S_u(\omega))\,\hat{\xi}_{ij}(\omega,n-1)\\ &\quad + Lz^2(\omega,n)S_u(\omega)S_{x_{ij}}(\omega) + S_{\check{h}_{ij}}(\omega),\end{aligned} \tag{36}$$

where $z(\omega,n)$ is the element in the diagonal of $\frac{1}{L}\mathbf{F}\mathbf{Z}(n)\mathbf{F}^H$. Furthermore, we can show from Eqs. (32) and (33) that

$$z(\omega,n) = \frac{1-\lambda}{S_u(\omega)}, \tag{37}$$

when-ever the matrix $\mathbf{P}(n)$ has converged.

Finally, using Eqs. (36), (19) and (37), the PTF estimate is

$$\begin{aligned}\hat{\xi}(\omega,n) &= (2\lambda - 1)\,\hat{\xi}(\omega,n-1)\\ &\quad + L\frac{(1-\lambda)^2}{S_u(\omega)}\sum_{i=1}^{P}\sum_{j=1}^{P} G_i(\omega)G_j^*(\omega)S_{x_{ij}}(\omega)\\ &\quad + \sum_{i=1}^{P}|G_i(\omega)|^2 S_{\check{h}_{ii}}(\omega).\end{aligned} \tag{38}$$

5. INTERPRETATION

5.1 PTF for NLMS Algorithm

Considering Eq. (29) as a first-order difference equation in $\hat{\xi}(\omega,n)$, the convergence rate of the cancellation system when using the NLMS algorithm is determined by

$$\alpha = 1 - 2\frac{\mu(n)}{L\sigma_u^2}S_u(\omega). \tag{39}$$

From Eq. (39), we observe that the loudspeaker signal $u(n)$ has an influence on the convergence rate. This is also the case when using the LMS algorithm, see Eq. (22). However, the convergence rate is now directly proportional to the ratio between $S_u(\omega)$ and σ_u^2. Changes of the absolute level of the PSD $S_u(\omega)$ at all frequencies would no longer have any effects on the convergence rate which is the case when using the LMS algorithm, but the shaping of the PSD $S_u(\omega)$ would lead to variations in the convergence rate.

According to Eqs. (39) and (24), the value of the step size $\mu(n)$ to ensure system stability is

$$0 < \mu(n) < \frac{L\sigma_u^2}{\max_\omega S_u(\omega)}. \tag{40}$$

Furthermore, we can determine the steady-state behavior as

$$\begin{aligned}\hat{\xi}(\omega,\infty) &= \lim_{n\to\infty} \hat{\xi}(\omega,n) \\ &= \underbrace{\lim_{n\to\infty} \frac{\mu(n)}{2\sigma_u^2} \sum_{i=1}^{P}\sum_{j=1}^{P} G_i(\omega)G_j^*(\omega)S_{x_{ij}}(\omega)}_{\text{Steady-State Error}} \\ &\quad + \underbrace{\lim_{n\to\infty} L\sigma_u^2 \frac{\sum_{i=1}^{P}|G_i(\omega)|^2 S_{\tilde{h}_{ii}}(\omega)}{2\mu(n)S_u(\omega)}}_{\text{Tracking Error}},\end{aligned} \tag{41}$$

where the first part is the steady-state error, when the feedback paths remain time-invariant. If the feedback paths undergo changes over time, an extra error contribution is introduced to the steady-state behavior, as a tracking error, which is represented by the second part of Eq. (41).

To summarize, a large step size $\mu(n)$ gives advantageously higher convergence rate and better tracking ability when feedback paths vary over time. However, the price paid is the increased steady-state error. Furthermore, the ratio $S_u(\omega)/\sigma_u^2$ is directly proportional to the convergence rate and tracking ability of changing acoustic feedback paths, whereas the length L of the estimated feedback path has the opposite effect. The PSDs $S_{x_{ij}}(\omega)$ of the incoming signals weighted by the frequency responses $G_i(\omega)$ and $G_j^*(\omega)$ of the beamformer filters are directly proportional to the steady-state error, whereas the loudspeaker signal variance σ_u^2 affects it inversely.

Using Eq. (39), we can achieve a desired convergence rate by choosing the step size according to

$$\mu(n) = L\sigma_u^2 \frac{1-\alpha}{2S_u(\omega)}. \tag{42}$$

From Eq. (41), a desired steady-state value of $\hat{\xi}(\omega,\infty)$, ignoring the feedback path variations for simplicity, can be achieved by choosing the step size according to

$$\mu(n) = \frac{2\sigma_u^2\hat{\xi}(\omega,\infty)}{\sum_{i=1}^{P}\sum_{j=1}^{P} G_i(\omega)G_j^*(\omega)S_{x_{ij}}(\omega)}. \tag{43}$$

5.2 PTF for RLS Algorithm

Similar to the NLMS case, the convergence rate for the RLS algorithm is determined from Eq. (38) as

$$\alpha = 2\lambda - 1. \tag{44}$$

This means that not only is the convergence rate frequency independent, but it is also signal independent; only the forgetting factor λ has influence on it. This differs completely from the LMS and the NLMS algorithms.

From Eqs. (44) and (24), we can determine the range of the forgetting factor λ to ensure the system stability as

$$0 < \lambda < 1. \tag{45}$$

Finally, the steady-state behavior is determined by

$$\begin{aligned}\hat{\xi}(\omega,\infty) &= \lim_{n\to\infty} \hat{\xi}(\omega,n) \\ &= \underbrace{L\frac{1-\lambda}{2S_u(\omega)} \sum_{i=1}^{P}\sum_{j=1}^{P} G_i(\omega)G_j^*(\omega)S_{x_{ij}}(\omega)}_{\text{Steady-State Error}} \\ &\quad + \underbrace{\frac{\sum_{i=1}^{P}|G_i(\omega)|^2 S_{\tilde{h}_{ii}}(\omega)}{2(1-\lambda)}}_{\text{Tracking Error}}.\end{aligned} \tag{46}$$

From Eq. (46), we observe another major difference compared to the LMS and NLMS algorithms. The PSD $S_u(\omega)$ of the loudspeaker signal is inversely proportional to the steady-state error of the system with time invariant feedback paths, and it has no influence on the additional tracking error caused by time-varying feedback paths.

We conclude that decreasing the forgetting factor λ increases the convergence rate and the tracking ability of the feedback path variations, but it increases the steady-state error as well. Furthermore, the length L of the estimated feedback paths, as well as the PSDs $S_{x_{ij}}(\omega)$ weighted by $G_i(\omega)$ and $G_j^*(\omega)$ are directly proportional to the the steady-state error.

Using Eq. (44), we can obtain a desired convergence rate by choosing the forgetting factor according to

$$\lambda = \frac{1+\alpha}{2}. \tag{47}$$

From Eq. (46), a desired steady-state value of $\hat{\xi}(\omega,\infty)$, ignoring again the feedback path variations for simplicity, can be achieved by choosing the step size according to

$$\lambda = 1 - \frac{2S_u(\omega)\hat{\xi}(\omega,\infty)}{L\sum_{i=1}^{P}\sum_{j=1}^{P} G_i(\omega)G_j^*(\omega)S_{x_{ij}}(\omega)}. \tag{48}$$

5.3 Statistically Identical Systems Behavior

By choosing the step sizes $\mu_0(n)$ and $\mu(n)$ according to Eq. (28), we can obtain statistically identical system behaviors in terms of the convergence rate and steady-state behavior, at all frequencies, for the LMS and the NLMS algorithms.

More interestingly, it is also possible to obtain statistically identical system behaviors when using the NLMS and RLS algorithms. We can derive the relation between $\mu(n)$ and λ to obtain this, e.g. from Eqs. (39) and (44), as

$$\mu(n) = \frac{L\sigma_u^2(1-\lambda)}{S_u(\omega)}. \tag{49}$$

Though, in general, this is only possible at a specific frequency, unless the PSD $S_u(\omega)$ is (partly) flat.

6. EXPERIMENTS

We conduct two simulation experiments, based on an MMSL system with $P = 3$ microphones, to verify Eqs. (39), (41)-(43) for the NLMS algorithm, and Eqs. (44), (46)-(48) for the RLS algorithm.

The same simulation procedures are used in both experiments. In each simulation run, the incoming signals $x_i(n)$ and the loudspeaker signal $u(n)$ are new realizations of Gaussian white noise sequences shaped by first-order FIR shaping filters $\mathbf{h}_{x_1}(n) = [1, 0.3]^T$,

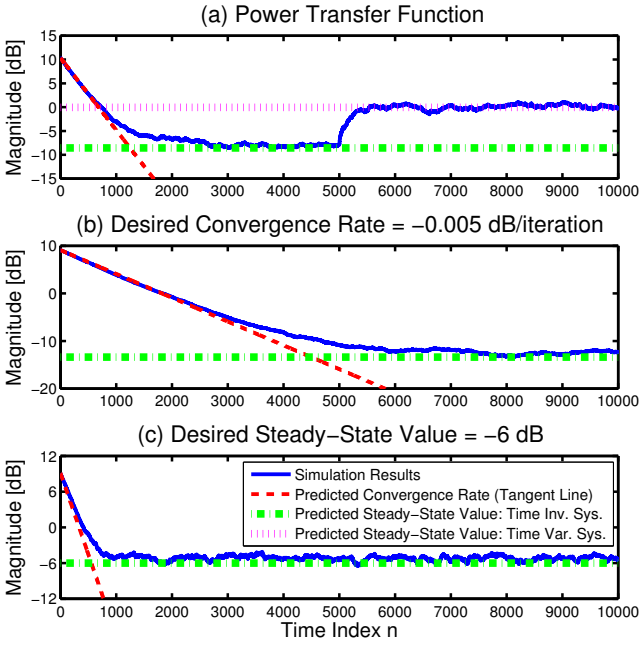

Figure 2: NLMS algorithm: the simulation results and the predictions using Eqs. (a) (39) and (41). (b)-(c) (42)-(43).

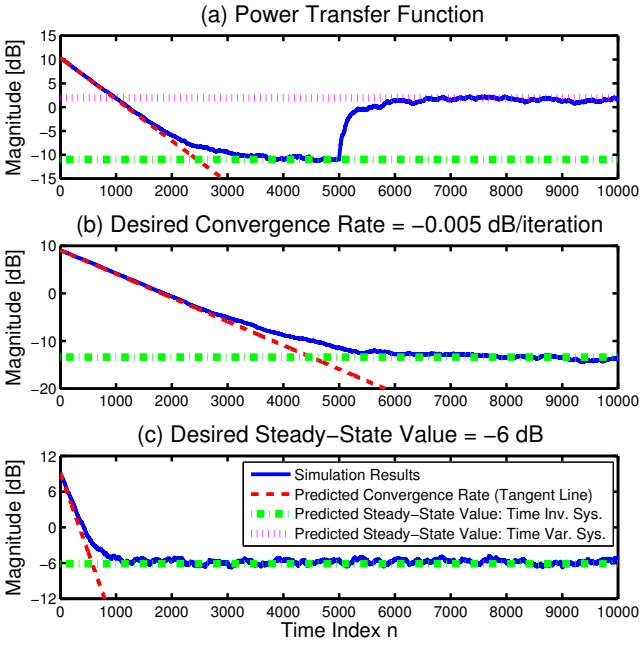

Figure 3: RLS algorithm: the simulation results and the predictions using Eqs. (a) (44) and (46). (b)-(c) (47)-(48).

$\mathbf{h}_{x_2}(n) = [1, -0.2]^T$, $\mathbf{h}_{x_3}(n) = [1, 0.5]^T$ and $\mathbf{h}_u(n) = [1, -0.3]^T$, respectively. The beamformer filters $\mathbf{g}_i$ and the feedback path filters $\mathbf{h}_i(n)$ are modeled as fixed first-order FIR filters $\mathbf{g}_1 = [1, 0.36]^T$, $\mathbf{g}_2 = [1, -0.32]^T$, $\mathbf{g}_3 = [1, 0.23]^T$, $\mathbf{h}_1(n) = [1, 0.14]^T$, $\mathbf{h}_2(n) = [1, -0.4]^T$ and $\mathbf{h}_3(n) = [1, 0.21]^T$, respectively. The verification of the predicted results using the derived expressions is possible because we know the true feedback paths $\mathbf{h}_i(n)$. Hence, we can use Eqs. (18), (8), (9) and (11) to compute the true PTF from the simulations. In both experiments, 100 simulation runs are performed to obtain an averaged $\xi(\omega, n)$, and each simulation run has a duration of 10^4 iterations. The initial feedback path estimates are $\hat{\mathbf{h}}_i(0) = \mathbf{0}_{L\times 1}$, where $L = 32$.

In the first experiment, the true feedback paths are fixed during the first half of the simulations, whereas random walk variations with variances $\sigma^2_{h_1} = 0.0384$, $\sigma^2_{h_2} = 0.0332$ and $\sigma^2_{h_3} = 0.0024$ are added during the second half. A fixed step size $\mu(n) = 2^{-4}$ is used for the NLMS algorithm, whereas a forgetting factor $\lambda = 0.999$ is used for the RLS algorithm.

The simulated and predicted results, at a representative example frequency $\omega = 2\pi l/L$, where $l = 7$, are shown in Figs. 2(a) and 3(a), respectively. In both cases, the simulation results confirm the predicted convergence rate and steady-state behavior with/without the feedback path variations. Furthermore, despite the underlying asymptotic assumptions of $L \to \infty$, $\mu(n) \to 0$ and $\lambda \to 1$ in the analysis, we observe that the derived expressions are accurate for practical values as $L = 32$, $\mu(n) = 2^{-4}$ and $\lambda = 0.999$.

In the second experiment, for the NLMS algorithm, we use Eqs. (42)-(43) to compute the step size $\mu(n)$ to achieve a desired convergence rate of -0.005 dB/iteration and a steady-state value of -6 dB, respectively. Similarly, for the RLS algorithm, we use Eqs. (47)-(48) to determine the forgetting factor λ to achieve the same behaviors. The feedback paths are fixed in this experiment, otherwise the same settings as in the first experiment are used.

The simulated and predicted results at the frequency bin $l = 7$ are shown in Figs. 2(b)-(c) and 3(b)-(c), respectively. Again, the simulation results confirm the derived expressions.

Furthermore, the statistically identical behaviors demonstrated in Figs. 2(b)-(c) and 3(b)-(c) can be explained by the fact that $\mu(n)$ and λ were chosen in accordance with Eq. (49).

7. CONCLUSIONS

In this work, we extended our previous work [4] based on the LMS algorithm. Specifically, we derived analytic expressions for the convergence rate, system stability bound and the steady-state behavior, in terms of the power transfer function, when using the NLMS and RLS algorithms for acoustic feedback/echo cancellation, in a multiple-microphone and single-loudspeaker system with a beamformer. Furthermore, we demonstrated that with an appropriate step size choice, the LMS and NLMS algorithms are statistically identical, whereas the behavior of the RLS algorithm is generally different than the LMS and NLMS algorithms, and we identified conditions for obtaining statistically identical behaviors for the NLMS and RLS algorithms.

REFERENCES

[1] J. Benesty, T. Gänsler, D. R. Morgan, M. M. Sondhi, and S. L. Gay, *Advances in Network and Acoustic Echo Cancellation*. Springer Verlag, 2001.

[2] T. van Waterschoot and M. Moonen, "Fifty years of acoustic feedback control: state of the art and future challenges," *Proc. IEEE*, vol. 99, no. 2, pp. 288–327, 2011.

[3] S. Haykin, *Adaptive Filter Theory*. Prentice Hall, 4th ed., September 2001.

[4] M. Guo, T. B. Elmedyb, S. H. Jensen, and J. Jensen, "Analysis of adaptive feedback and echo cancelation algorithms in a general multiple-microphone and single-loudspeaker system," in *Proc. 2011 IEEE Int. Conf. Acoust., Speech, Signal Process.*, pp. 433–436.

[5] S. Gunnarsson and L. Ljung, "Frequency domain tracking charateristics of adaptive algorithms," *IEEE Trans. Acoust., Speech, Signal Process.*, vol. 37, pp. 1072–1089, July 1989.

[6] H. Nyquist, "Regeneration theory," *Bell System Technical Journal*, vol. 11, pp. 126–147, 1932.

[7] R. M. Gray, *Toeplitz and Circulant Matrices: A Review*. Now Publishers Inc, January 2006.